GeoStudies

GeoStudies 2: 35–49 (2025)
DOI: 10.3897/geostudies.2.e126114

Research Article

Magnetic effects of disjunctive thin layers in 2D forward models and their equivalent magnetic sources

Petar Stavrev[1], Petya Trifonova[2], Metodi Metodiev[2]

1 *University of Mining and Geology "St. Ivan Rilski", Sofia, Bulgaria*
2 *National Institute of Geophysics, Geodesy and Geography – Bulgarian Academy of Sciences, Sofia, Bulgaria*
Corresponding author: Petya Trifonova (ptrifonova@geophys.bas.bg)

Abstract

Analysis and solution of the forward magnetic problem for models of disjunctive layered geological structures, such as faults and layer discontinuities, are developed in this paper. Magnetic anomaly components Z, H, T, ΔT and Ta resulting from disjunctive geologic structures are similar to those caused by thin-layer magnetic sources of finite size. Structures of a discontinuous horizontal layer, an up-thrown fault, inclined, normal or reverse faulted, an over-thrusted structure and also a thick-layer fault of the relatively small throw are examined. The composition of different forward magnetic models of disjunctive structures and their calculations can be facilitated by the applied specific properties of thin layers with unlimited depth extent. A method of rotation is proposed to analyse the anomalous magnetic effects caused by discontinuous crustal structures. The results shown are useful in analysing field magnetic data, recognising sources, inverting anomalies and interpreting geophysical data.

Key words: Magnetic anomalies, forward modelling, 2-D structures, equivalent compact source, analytical expressions

OPEN ACCESS

Academic editor:
Maria Kostadinova-Avramova
Received: 24 April 2025
Accepted: 17 March 2025
Published: 30 May 2025

Citation: Stavrev P, Trifonova P, Metodiev M (2025) Magnetic effects of disjunctive thin layers in 2D forward models and their equivalent magnetic sources. GeoStudies 2: 35–49. https://doi.org/10.3897/geostudies.2.e126114

Copyright: © Petar Stavrev et al.
This is an open access article distributed under terms of the Creative Commons Attribution License (Attribution 4.0 International – CC BY 4.0).

Introduction

Magnetic methods in exploration geophysics are based on using contrasts in magnetisation between different lithologies or magnetic sources of other origin; they are used to solve geological, environmental, mining, archaeological and other problems. Recent examples can be found in Grauch et al. (2001, 2006), Eppelbaum (2015), Dimovski et al. (2017, 2020), Dar and Bukhari (2020) and Essa and Abo-Ezz (2021). Interpretation of magnetic anomalies using model sources with simple geometric shape, like those analysed here below, may reduce the complexity of inverse problems and offer usable best-fit solutions.

According to the theory of physical fields as applied to exploration geophysics, a horizontal layer having constant magnetisation, finite thickness and infinite size in all horizontal directions creates a homogeneous magnetic field only inside the layer, while, outside the source region, the field intensity is equal to zero (Telford et al. (1990) see for example, Stavrev and Radichev (2015)). If the horizontal layer is of finite size or has discontinuity anywhere, then the magnetic field appears outside the source region as well.

In this case, respective forward and inverse problems can have solutions. The next parts of this paper show the construction of the appropriate 2D models and discuss their specific properties.

Forward 2D problem for disjunctive structures of thin layers under magnetisation

The main phases in a forward 2D problem, as applied here, are as follows: (P1) Choice of shapes for the basic elements of a 2D structure; (P2) Determination of the location and parameters of inductive magnetisation for a 2D model elements; (P3) Calculation of magnetic field created by basic elements of a structure using analytical expressions; (P4) Assignment of a given 2D structure in vertical cross-section; (P5) Calculations of its magnetic effects; (P6) Analysis of results regarding equivalent sources of magnetic effects.

(P1): In the initial phase of selecting a basic element, we consider a model of a homogeneous, thin geological layer with a rectangular cross-section. This layer is envisioned in a vertical two-dimensional plane beneath the Earth's surface, featuring a small cross-section and extending infinitely in length (see examples shown in figures below). The model also allows the formation of spatially limited thin elements of finite length.

(P2): For this task, a generalised spatial scenario has been established for the placement and description of a magnetic 2D layered model, as illustrated in Figure 1.

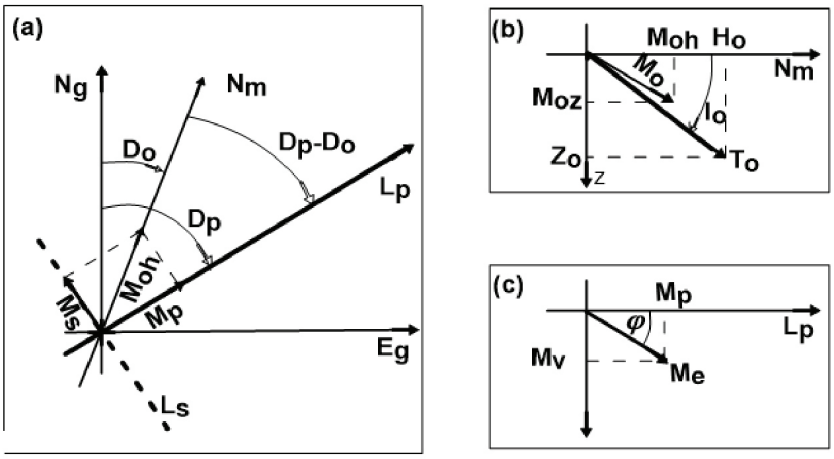

Figure 1. (**a**) Line L_p of a magnetic profile across the strike L_s of a thin-layer structure. Symbols are as follows: N_g – geographic North, E_g – geographic East, N_m- magnetic North, D_0 – declination of the normal geomagnetic field, D_p – geographic azimuth of L_p, (D_p-D_0) – magnetic azimuth of L_p, M_{0h} – horizontal component of inductive magnetisation, M_p – projection of M_{0h} along profile line L_p, M_s – projection of M_{0h} along line L_s; (**b**) The vertical plane of the magnetic meridian N_m, symbols stand for: I_0 – the inclination of the normal geomagnetic field, M_{0z} and M_{oh} – vertical and horizontal components of inductive magnetisation M_0; (**c**) Vertical plane of magnetic profile line L_p, symbols standing for M_v, M_p – vertical and horizontal components of the effective inductive magnetisation M_e, φ – dip angle of M_e

Using mathematical notations and symbols from Fig. 1, the horizontal M_{oh} and vertical M_{oz} components of the induced magnetisation are:

$$M_{0h} = \frac{k}{1+kf_h} H_0, M_{0z} = \frac{k}{1+kf_z} Z_0 \quad (1)$$

where k is the layer's magnetic susceptibility, f_h and f_z are demagnetising factors ranging between 0 and 1 in SI units. In our case, of horizontal thin layer f_h=0 for the horizontal component and f_z=1 for the vertical component (across the thin layer). H_0 and Z_0 are the horizontal and vertical components of the normal geomagnetic field. Thus, the magnetisation induced by the source body can be expressed by:

$$M_{0h} = kH_0, M_{0z} = \frac{k}{1+k} Z_0, \quad M_0 = \sqrt{{M_{0h}}^2 + {M_{0z}}^2} = k\sqrt{{H_0}^2 + \frac{{Z_0}^2}{(1+k)^2}} \quad (2)$$

Following (2), the effective magnetisation M_e has the components,

M_{0z} (shortened symbol $M_v = M_{0z}$ in Fig. 1c) and $M_{0h}\cos(D_p - D_0) = M_p$ (Fig. 1a and 1c). (3)

The component M_s along the strike does not create a magnetic effect. Thus, after simple rearrangement of equations (2) and (3), the analytical expressions for effective magnetisation M_e become:

$$M_e = \sqrt{{M_v}^2 + {M_p}^2} = kH_0 \cos(D_p - D_0)/\cos\varphi, \quad \varphi = \tan^{-1}\left[\frac{1}{1+k} \cdot \frac{\tan I_0}{\cos(D_p - D_0)}\right] \quad (4)$$

In case of known remanent magnetisation, its components in vertical direction and along profile line L_p should be added algebraically to the respective components M_v and M_p.

(P3) Regarding the use of analytical expressions for the anomalous magnetic field, created by a thin layer under inductive magnetisation, we may see theoretical solutions in Logachev & Zaharov (1973), Tyapkin (1973), Telford et al. (1990), Blakely (1995) and Reid (2003). The theoretical problem in this case involves a two-dimensional magnetic field created by "flat" sources. The logarithmic potential and its derivatives have to be used to determine the intensity components of the magnetic field (see, for example, Dimitrov & Stavrev (1986)). Its sources are described within the plane formed by the horizontal *X*-axis and vertical *Z*-axis.

If the vector of effective magnetisation has been defined by its magnitude and dip angle according to (1) - (4), the components of the anomalous field can be calculated from the expressions:

$$Z = 2|M_e|t\frac{h\cos\theta - x\sin\theta}{x^2+h^2}, \qquad H = -2|M_e|t\frac{h\sin\theta + x\cos\theta}{x^2+h^2} \quad (5)$$

where angle $\theta = \alpha - \varphi$, angle α is the layer dip angle, φ is the magnetisation dip angle; t is the layer thickness; h is the depth of the layer edge; x is the horizontal coordinate of observation point $P(x,0)$ with respect to the layer edge $E(0,h)$ in the 2D *XOZ* coordinate system. Axis *X* runs from left to right and axis *Z* is pointed downwards. Angles α and φ should be taken from the positive direction of axis *X* clockwise from 0 to 360 degrees. The formula (5), shown by Logachev & Zaharov (1973) with multiplier sin(α) on right side of the two above expressions, are designed for thin layer models with apparent thickness. Here, we make use of the strong rectangular shape of layer models (see P1).

After calculating the vertical and horizontal magnetic components Z and H, the anomalous total magnetic intensity ΔT (F) can be determined by an approximation. We find its additive and quasi-harmonic approximation useful for this purpose in case of a moderate anomalous field (see, for example, Cady (1980); Blakely (1995)). In addition, the magnitude of the full anomalous vector T can be calculated as:

$$\Delta T = Z \sin I_0 + H \cos I_0 \cos(D_P - D_0)\,; \qquad T = (Z^2 + H^2)^{1/2} \tag{6}$$

The results from calculations for the magnetic anomalies of a thin layer of a semi-infinite length have been analysed for three characteristic positions of the layer. It has been established that, for each component of the created magnetic field, the same values are maintained at a constant angular difference (θ) between the layer inclination (α) and the magnetisation vector (φ). Additionally, while the sign of the angle θ changes, the shapes of the curves Z and H also change, but the total intensity T remains consistent in both form and value (see Figs. 2 a, b and c). This unique property of the magnetic effect of a thin layer could be beneficial for solving both forward and inverse problems.

(P4): The 2D model of a given disjunctive structure assumes the existence of two thin layers as a result from the separation of continuously existing

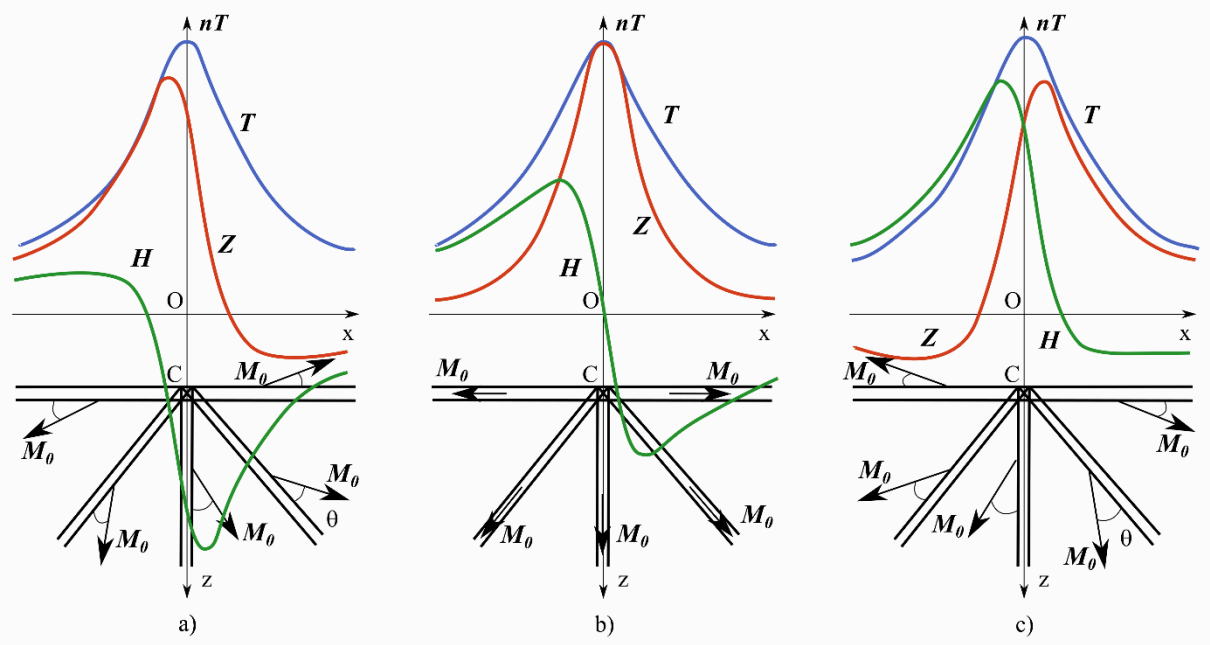

Figure 2. Anomalies Z, H and T of thin-bed structures with infinite extent. Each case shows thin layers with the same magnetic parameters, but with different strike (horizontal, inclined and vertical). The three cases have different conditions for the angle θ as follows: a) $\theta > 0$; b) $\theta = 0$; c) $\theta < 0$; (after Dimitrov & Stavrev (1986)).

thin layers within space. The geological and physical appearance indicates the emergence of two distinct thin layers, each exhibiting its own magnetic effects, based on the same magnetic properties discussed above. They should be estimated and put in a summation to determine the resulting magnetic anomaly. The complicated forward modelling of such discontinuous thin layers could be facilitated by the rotation method proposed here, due to

specific properties of the magnetic fields, created by thin layers. Analytical equations (5) and (6) include two types of variables – space geometrical *x, h, t* angle *a,* and magnetic variables M_e and its angle *φ*. The two angles enter the trigonometric functions in equations (5) as their difference, *θ = α − φ*. If a thin layer has an upper point *C* and extends semi-infinitely in the subsurface space at angles *θ* and *φ*, then when the layer rotates around centre *C*, while maintaining a constant angle *θ*, the magnetic anomaly effect it generates will remain constant along the magnetic profile of the observation points. This specific formal property is illustrated in Figure 2 and also in the next figures of 2D disjunctive structures. When calculating the common magnetic effect, if the two layers participate in that process, it is possible to obtain an active component between them using the method of rotation layers with equal magnetic effects (see Figs. 2 and 3 and demonstrated models later on). The active component consists of a single thin layer positioned between the two thin magnetic layers whose magnetisation is in the direction obtained by rotating both magnetic layers about their inner edges. The upper (or left) magnetic layer is rotated in an anti-clockwise direction, while the lower layer is rotated in a clockwise direction, until both layers align with the line connecting their original positions. As a result, the only part that is magnetically active lies along the original gap, while the area beneath the lower part produces zero effect due to the opposite directions of their vectors of magnetisation.

(P5): The above concept allows us to utilise established analytical expressions for the magnetic effects of a finite active layer. Therefore, the empty space between the two thin layers in a disjunctive structure can be represented as a material equivalent to one of the layers during the rotation process. We can interpret this residual section as a finite equivalent 2D magnetic source of the disjunctive structure. Consequently, solving the forward magnetic problem can be simplified to calculating the magnetic anomalies generated by a thin layer of finite length.

Analytical expressions for the anomalous magnetic field of thin layers that are limited in length resemble the formulae (5) and (6). The coordinate system is defined with axes *XOZ* positioned above the mid-point of the horizontal or inclined limited layer (Fig. 3). Its parameters are as follows: depth (*h*), length (*2l*), inclination angle (*α*), thickness (*t*), magnetisation M_e at angle *φ*, angle *θ = α - φ*.

Sums $Z = Z_1 + Z_2$ and $H = H_1 + H_2$ can be determined using the following expressions:

$$Z_1 = 2M_e t\frac{(h-l\sin\alpha)\cos\theta-(x+l\cos\alpha)\sin\theta}{(x+l\cos\alpha)^2+(h-l\sin\alpha)^2},\ Z_2 = -2M_e t\frac{(h+l\sin\alpha)\cos\theta-(x-l\cos\alpha)\sin\theta}{(x-l\cos\alpha)^2+(h+l\sin\alpha)^2} \quad (7)$$

$$H_1 = -2M_e t\frac{(h-l\sin\alpha)\sin\theta+(x+l\cos\alpha)\cos\theta}{(x+l\cos\alpha)^2+(h-l\sin\alpha)^2},\ H_2 = 2M_e t\frac{(h+l\sin\alpha)\sin\theta+(x-l\cos\alpha)\cos\theta}{(x-l\cos\alpha)^2+(h+l\sin\alpha)^2} \quad (8)$$

$$\Delta T = (Z_1 + Z_2)\sin I_0 + (H_1 + H_2)cosI_0\cos\left(D_p - D_0\right),\ T_a = (Z^2 + H^2)^{1/2} \quad (9)$$

Analytical expressions for calculating the anomalous magnetic effect of a limited layer can be derived directly using the coordinates (x_{01}, h_1) and (x_{02}, h_2) without needing to specify the mid-point and length of the layer.

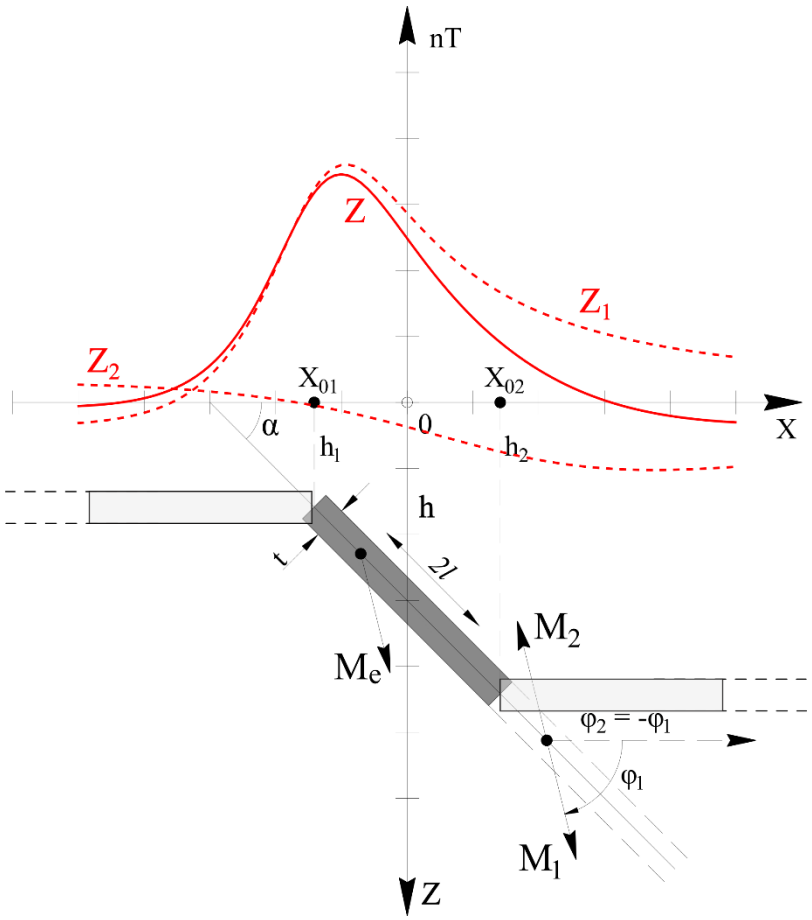

Figure 3. Representation of the anomalous effect $Z = Z_1 + Z_2$ from a limited thin layer as a combination of two layers unlimited in depth with an inclination angle (α) and thickness (t), but at a different starting points with coordinates (x_{01}, h_1) and (x_{02}, h_2) and having oppositely directed magnetisation vectors M_1 and M_2. Thus, for the limited layer, the magnetisation vector $M_e = M_1$ is obtained and, for the second, deeper layer, the effective vector magnetisation is $M_2 - M_1 = 0$.

P(6): An analysis of the above expressions and results, regarding *Z* and *H* magnetic anomalies, shows that they contain, in addition to (5), one more length parameter denoted as *l* after the first multiplier $2M_e t$ with thickness parameter *t*. This fact provides the physical sense of magnetic effects from disjunctive structures and their sources. This important conclusion is analysed in the next part of this paper.

Magnetic effects from magnetised thin layers in disjunctive structures

Note: *The magnetic profiles of the studied structures strike from west to east in the northern geomagnetic hemisphere at latitude around 40°N and longitude around 20°E. The inclination of the normal geomagnetic field is close to 60° with a declination around 5°.*

1.Offset of a 2-D horizontal thin layer (Fig. 4)

This is a typical example of the simplest model structure for analysis. We have two magnetic layers separated horizontally at a relatively small distance (Fig. 4b).

The anomalous field components Z and H can be represented as a sum of respective components caused by both thin layers: number '1' from the left and number '2' from the right side of the braked structure. The zero point of the horizontal x-axis is chosen in the mid-point of the structure and the zero point of the downward z-axis is in the line of observation point $P(x,0)$. The horizontal offset is denoted here by the symbol w. Thus, the coordinates of the edge points of the two layers are $E_1(x+w/2, z_1)$ and $E_2(x-w/2, z_2)$. According to the expression (5), we may write:

$$Z = Z_1 + Z_2 = 2M_0\, t\left(\frac{h_1\cos\theta_1 - x_1\sin\theta_1}{x_1^{\,2} + h_1^{\,2}} + \frac{h_2\cos\theta_2 - x_2\sin\theta_2}{x_2^{\,2} + h_2^{\,2}}\right) \tag{10}$$

$$H = H_1 + H_2 = -2M_0\, t\left(\frac{h_1\sin\theta_1 + x_1\cos\theta_1}{x_1^{\,2} + h_1^{\,2}} + \frac{h_2\sin\theta_2 + x_2\cos\theta_2}{x_2^{\,2} + h_2^{\,2}}\right) \tag{11}$$

where $x_1 = x + w/2$, $x_2 = x - w/2$, $h_1 = z_1$, $h_2 = z_2 = z_1$, $h_1 = h_2 = h$,
$\theta_1 = \alpha_1 - \varphi_1 = 180° - \varphi$, $\theta_2 = \alpha_2 - \varphi_2 = 0° - \varphi$, $\varphi_1 = \varphi_2 = \varphi$
φ is the dip angle of effective layers magnetization M_0, t is the layers' thickness.

After an algebraic summation of Z_1 and Z_2, we obtain the complicated expression:

$$Z = Z_1 + Z_2 = 2M_0\, t\,\frac{w\left[(x^2 - h^2)\sin\varphi + 2xh\cos\varphi - (w/2)^2\sin\varphi\right]}{(x^2 + h^2)^2 - 2(x^2 - h^2)(w/2)^2 + (w/2)^4} \tag{12}$$

The coefficient M_0t above could be multiplied by $(w/w=1)$ in order to form the coefficient $(M_0tw)/w$. The offset size w in the denominator of $(M_0tw)/w$ eliminates the appearance of size w in the numerator of equation (12). The rest of the above coefficient is $M_0tw = m_0$. Thus we obtain for Z:

$$Z = 2m_0\,\frac{(x^2 - h^2)\sin\varphi + 2xh\cos\varphi - (w/2)^2\sin\varphi}{(x^2 + h^2)^2 - 2(x^2 - h^2)(w/2)^2 + (w/2)^4} \tag{13}$$

In the same way, the result for the horizontal components sum $H = H_1 + H_2$ is

$$H = -2m_0\,\frac{(x^2 - h^2)\cos\varphi - 2xh\sin\varphi - (w/2)^2\cos\varphi}{(x^2 + h^2)^2 - 2(x^2 - h^2)(w/2)^2 + (w/2)^4} \tag{14}$$

In the above two equations of the total intensity, the coefficient $M_0tw = m_0$ has, as a physical quantity, the dimension [(Tesla) x (m) x (m)] = [Tm^2], where m^2 gives geometrically the area of the finite layer with size tw and M_0 is the magnitude of the magnetic factor. Thus, the numerical value of the coefficient m_0 is equal to the modulus of the magnetic moment of the finite equivalent layer per unit length along the Y axis in the 2D model. This justifies taking the finite layer as an equivalent source of the anomalous magnetic effect.

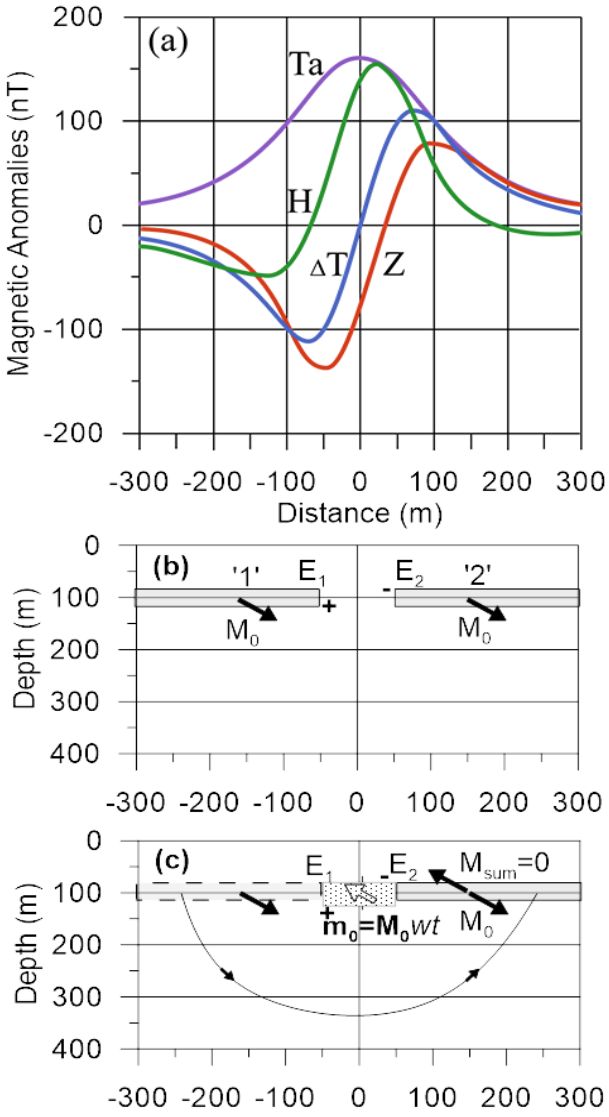

Figure 4. (**a**) Magnetic anomalies ΔT, Z, H and T_a caused by the discontinuous (broken) layer structure of two thin layers shown in (**b**) with magnetisation vector M_0 with angle φ = 30^0, (**c**) equivalent source of limited length (in dotted pattern) with 2-D magnetic moment $\boldsymbol{m}_0$ under angle φ = 180^0+30^0 = 210^0 after the geometric rotation of the left layer '1' upon the right one '2'

If the width w of the structure is negligibly small with respect to the distances between the thin-layer and the observation points, then, according to equations (12) - (14), we may write:

$$Z = 2m_0 \frac{(x^2 - h^2)\sin\varphi + 2xh\cos\varphi}{(x^2 + h^2)^2}, \quad H = -2m_0 \frac{(x^2 - h^2)\cos\varphi - 2xh\sin\varphi}{(x^2 + h^2)^2} \tag{15}$$

$$\Delta T = 2m_0 \frac{(x^2 - h^2)S_w + 2xhC_w}{(x^2 + h^2)^2}, \qquad T_a = \sqrt{Z^2 + H^2} = 2m_0 \frac{1}{x^2 + h^2} \tag{16}$$

These expressions correspond to the well-known expressions (see, for example, Dimitrov & Stavrev (1986)) for the anomalous field caused by a 2-D line

of point dipoles having magnetic moment m_0. The example in Fig. 4c uses inclined magnetic moment and magnetisation.

The rotation method shown in Fig. 4c is used to analyse discontinuous crustal structures and their anomalous magnetic effects. This method can also be applied to other disjunctive structures with thin layers. Results in graphic form are given in Figs. 5, 6 and 7 below.

2. Vertical fault of a 2-D thin magnetic layer (Fig. 5)

3. Thick magnetic layer faulted with small displacement (throw) (Fig. 6)

4. Dipping fault of a thin layer (Fig. 7)

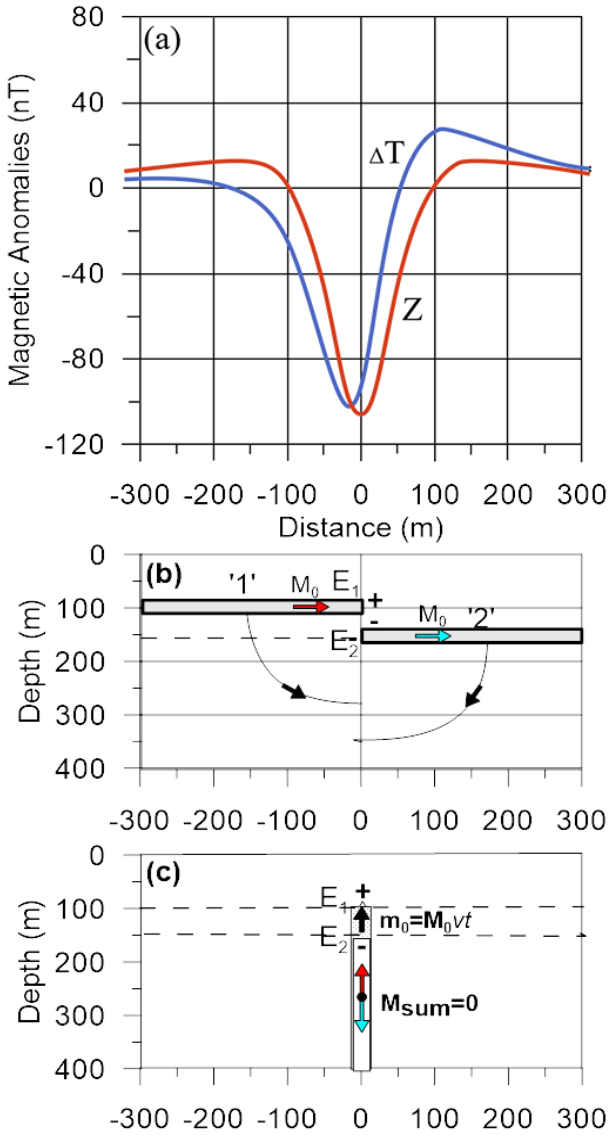

Figure 5. (**a**) Magnetic anomalies ΔT and Z caused by a fault structure of two thin layers shown in (**b**), with magnetisation $\mathbf{M}_0$; (**c**) Equivalent source between edge point E_1 and E_2 with magnetic moment $\mathbf{m}_0 = \mathbf{M}_0 vt$ is formed in its real position and sizes after geometric rotation of the layer '1'(left) and layer '2' (right) rotated up to the line joining + to - from both sides and obtaining vertical position, where the lower part of coincidence under point E_2 is not magnetically active because of vector sum $\mathbf{M}_{sum} = \mathbf{M}_{01} + \mathbf{M}_{02} = 0$. Magnetisation can have any desirable angle φ from 0 to 360^0. Fig. 3 illustrates a particular case of horizontal magnetisation (angle $\varphi = 0^0$).

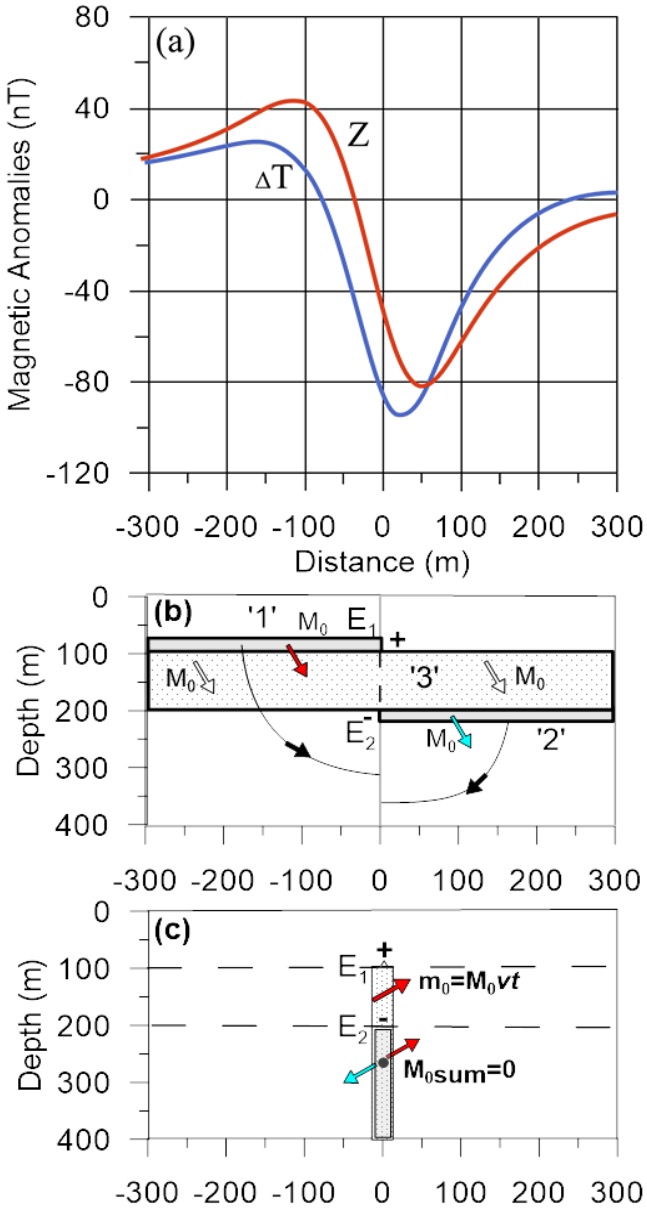

Figure 6. (**a**) Magnetic anomalies Δ*T* and *Z* caused by a thick layer fault structure; (**b**) small throw that forms two active thin layers, '1' and '2' and not active not limited layer '3', all with magnetisation $\mathbf{M}_0$; (**c**) Equivalent source between edge points E_1 and E_2 with magnetic moment $\mathbf{m}_0 = \mathbf{M}_0 vt$ after geometric rotation of the left and right active layers to the vertical position, part of layer's coincident under point E_2 is not magnetically active as $\mathbf{M}_0$sum = 0. Fig. 4 illustrates a particular case of dip angle $\varphi = 60^0$.

Field scenarios applicable to layered magnetic structures

Faults within sedimentary basins are often associated with minor linear magnetic anomalies. These anomalies can be due to differences caused by the tectonic alignment of sedimentary layers with contrasting magnetic characteristics or by secondary magnetisation created by geochemical activity along the fault zone. The former, for example, may explain all of the anomalies related to intrasedimentary faults observed in the Albuquerque Basin (Grauch et al. 2001), a large sediment-filled Basin that comprises the central part of the Rio Grande Rift in northern New Mexico.

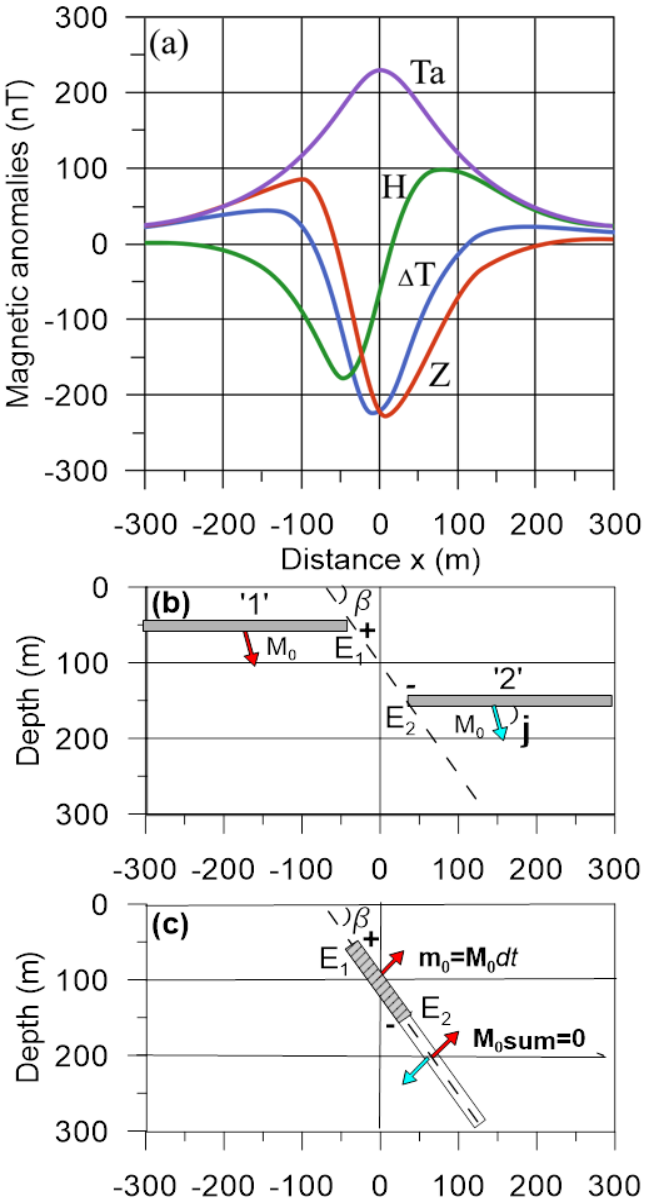

Figure 7. (**a**) Magnetic anomalies ΔT , Z , H and T_a caused by a dipping fault structure in (**b**) consisting of two thin layers with magnetisation $\mathbf{M}_0$; (**c**) Equivalent source (in raster of cross lines) with 2D magnetic moment $\mathbf{m}_0 = \mathbf{M}_0 dt$ after geometric rotation of the left bad and right layer to the dipping position under angle β, t is the thickness and d is the source length between edge points E_1 and E_2; the coinciding parts of the two layers under point E_2 compensate each other ($\mathbf{M}_0$sum = 0) so they are not magnetically active.

The linear anomalies in profiles show patterns typical of extensional faulting and all of them appear to be juxtapositions of layers with different magnetic properties (Grauch et al. 2001). Different curves are shown, ranging from a symmetric one expected over a contact to curves with two asymmetric peaks and two or more inflection points. These curves have amplitudes ranging from 2 to 40 nT (for data continued up to 100 m above ground). The magnetic curve over the Cat Mesa fault is best explained by magnetic layers offset along a fault, which is very similar to the theoretical case of a fault structure of two thin layers demonstrated in Figure 5. The San Ysidro Fault is another well-exposed fault in the central Rio Grande Rift, USA (Grauch et al. 2006). It is a significant fault within badlands

topography, allowing examination of varying structural depths along the strike. A linear anomaly ranging from 10 to 20 nT generally follows most of the fault's mapped extent, with some variations in anomaly shape along the strike.

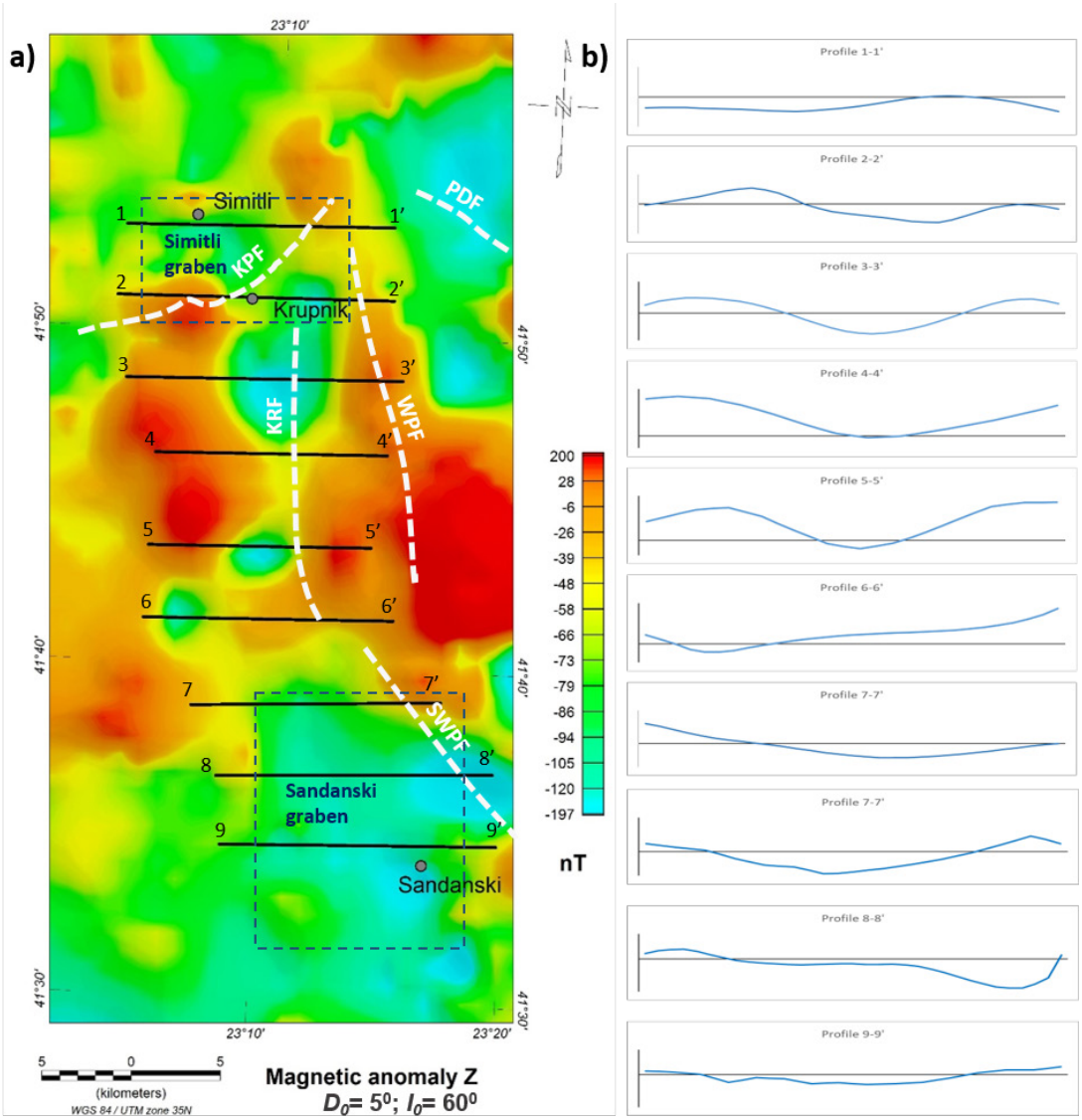

Figure 8. Magnetic anomaly map of the vertical component Za of the Strouma River valley (SW Bulgaria) characterised by extensive normal faulting, deposition of sediments and erosion of mountain ranges between the faults: KPF - Krupnik fault; KRF – Kresna fault; PDF – Predela fault; WPF – West-Pirin fault; SWPF – South-west Pirin fault. The positive anomalous group is caused by granite bodies locally enriched in ferromagnetic iron components at depths of 2-3 km. Continued normal faulting followed by partial remodelling of the sediment strata by rivers has formed typical magnetic anomalies caused by a thick layer fault structure inside the grabens (profiles 1-1', 2-2' and 9-9', 10-10') and vertical faults of a thin magnetic layer (profiles 3-3', 4-4' and 5-5').

It is clearly seen in the profile plots of Grauch et al. (2006) that most of the cases, especially in the northern part of the region, might be easily interpreted as discontinuous (broken) layer similar to structures of two thin layers shown in Fig. 4.

The territory of SW Bulgaria also has a complex tectonic structure with evidence for a composite fault mosaic. The diverse landscape is dominated by the modern valleys of Strouma and Mesta Rivers which developed their

fluviolacustrine systems after the late Eocene. Zagorcev (2007) found that the Late Cenozoic extension has been associated with normal faulting and deposition of sedimentary layers (> 1500 m in the Simitli and Sandanski Grabens). Further tectonism, characterised by increased normal faulting with unroofing of the Paleogene granite plutons in the highest horsts of Pirin and cyclic deposition of coarse sediments within the graben systems, led to progressive erosion of mountain ranges between normal faults. Under this condition, we can expect vertical or horizontal offsets of the strata, which will reflect the magnetic field and create anomalies similar to those studied here.

Figure 8 presents the residual vertical (Z) anomaly of the Strouma fault zone, a long and wide tectonic structure built by several parallel fault fractures. The clearly expressed anomalous group in the region is caused by granite bodies locally enriched in ferromagnetic iron minerals at depths of 2-3 km on average in the conditions of complicated fault tectonics. As already mentioned, Simitli and Sandanski Grabens are two of the numerous Tertiary grabens in this area developed along the Strouma River. They originate from the late Miocene over Precambrian metamorphites, Palaeozoic and Upper Cretaceous granites and are filled by Neogene sediments: sandstones, conglomerates clays and coal (Dobrev & Kostak 2000).

The highest horsts, including Osogovo, Rila, Pirin and Belasitsa, which surround the Strouma fault zone, experienced additional uplift during the Pleistocene. This uplift was partly due to regional tectonic activity and partly the result of ongoing normal faulting. As a consequence, the fluvial systems underwent partial remodelling, leading to the development of new gorges (Zagorcev 2007).

Interpretation of such anomalies, which are typical for faults within sedimentary basins can be simplified after applying the transformations described here. Usually, such magnetic anomalies over faulted strata are commonly caused by contrasts in the magnetisation intrinsic to the sediments that are juxtaposed at the fault.

Conclusions

In this paper, we show that the magnetic effect from disjunctive thin layers of infinite horizontal extension can be interpreted in terms of an equivalent source of finite size between edge points of the layers. It is demonstrated that a disjunctive thin layer of infinite horizontal extension creates an alternative magnetic source in the gap between the original layer's segments. This is a novel method for computing magnetic anomalies of offset magnetic layers using fewer parameters. Modelling of such a size-limited structure is done with a much simpler expression for the magnetic moment compared to the field of the two strike-unlimited layers.

With the graphical examples, we demonstrated that a small throw fault of a thick magnetic layer generates a magnetic anomaly resembling that of a thin-layer anomaly (compare the models shown in Fig. 6 and Fig. 7). The sign of the main extremum of the created magnetic anomaly can correspond to magnetisation in an opposite orientation to the normal layer's magnetisation direction, as illustrated in the model shown in Fig. 4.

Although we give real examples only for a sedimentary environment, the interpretation tips for two-dimensional horizontal infinite-length thin layers and

their discontinuities, like breaks or faults, might also apply to other layered geology, such as faulted volcanic flows.

The analysed anomalies of Z and ΔT which are based on forward models, as well as empirical observations gathered from real disjunctive geological structures, exhibit a notable predominance of negative and/or narrow anomalies. These negative anomalies are particularly intriguing as they can be traced across extensive distances, reflecting the intricate spread of elongated geological faults and disconnected structural elements within the Earth's crust. This phenomenon reveals a complex interplay of geological processes that influence the distribution and characteristics of subsurface formations.

Acknowledgements

We would like to thank the editor, Dr. Andrei Kosterov and the two anonymous reviewers for their significant engagement and comments, which helped us to improve the manuscript.

Additional information

Conflict of interest

Petar Stavrev and Metodi Metodiev declare no conflicts of interest. Petya Trifonova is a member of the editorial board of the Geosudies Journal.

Competing interests

The authors have no relevant financial or non-financial interests to disclose.

Ethical statement

No ethical statement was reported.

Funding

No funding was reported.

Author contributions

Petar Stavrev is the author who mainly contributed to the study's conception and model design. Material preparation and analysis were performed by Petar Stavre and Petya Trifonova. The first draft of the manuscript was proposed by Petar Stavrev, complemented and edited by Petya Trifonova. Metodi Metodiev contributed to the preparation of graphical materials. All authors commented on previous versions and key points of the discussion. All authors read and approved the final manuscript.

Author ORCIDs

Petya Trifonova https://orcid.org/0000-0002-9728-9984
Metodi Metodiev https://orcid.org/0000-0002-2950-9105

Data availability

All of the data that support the findings of this study are available in the main text.

References

Blakely RJ (1995) Potential theory in gravity and magnetic applications. Cambridge University Press, 435 pp. https://doi.org/10.1017/cbo9780511549816

Dimitrov LV, Stavrev PY (1986) Magnetic methods in geophysics. UMG Sofia, 434 pp. (in Bulgarian)

Dimovski S, Stoyanov N, Tzankov Ch, Kisyov At (2017) A geophysical approach for mapping of abandoned mining workings and unconsolidated zones in coal mining areas. Journal of Mining and Geological Sciences 60, Part 1: Geology and Geophysics: 99-103

Dimovski S, Stoyanov N, Tzankov Ch, Kisyov At (2020) Application of ERT method for localizing karst zones along the route of Balkan Stream gas pipeline, Bulgaria. Review of the Bulgarian Geological Society: 81 Part 3: 259-261.

Dobrev N, Kostak B (2000) Monitoring tectonic movements in the Simitli Graben, SW Bulgaria. Eng. Geol., 57, 179-192.

Eppelbaum, LV (2015). Quantitative interpretation of magnetic anomalies from bodies approximated by thick bed models in complex environments. Environmental Earth Sciences, 74, 5971-5988.

Grauch VJS, Hudson MR, Minor SA (2001) Aeromagnetic expression of faults that offset basin fill, Albuquerque basin, New Mexico. Geophysics 66(3): 707-720. https://doi.org/10.1190/1.1444961

Grauch VJS, Hudson MR, Minor SA, Caine JS (2006) Sources of along-strike variation in magnetic anomalies related to intrasedimentary faults: A case study from the Rio Grande Rift, USA. Exploration Geophysics 37(4): 372-378, https://doi.org/10.1071/EG06372

Hudson MR, Grauch VJS, Minor SA (2008) Rock magnetic characterization of faulted sediments with associated magnetic anomalies in the Albuquerque Basin, Rio Grande rift, New Mexico. GSA Bulletin:120 (5-6): 641–658. https://doi.org/10.1130/B26213.1

Logachev AA., Zacharov VP (1973) Magnetic exploration. 4th ed. Nedra Publishing House,350 pp (in Russian)

Stavrev P, Radithev R (2015) Theory of the physical fields in Exploration geophysics. MGU „St. Ivan Rilski" Publ. House, Sofia, Part (I,II) 274 pp (in Bulgarian)

Telford WM, Geldart LP, Sheriff RE (1990) Applied Geophysics. 2nd ed. Cambridge University Press, 770 pp.

Tyapkin KF (1973.Interpretation of Magnetic Anomalies Caused by Dikes and Contacts. Nedra Publishing House, 224 pp (in Russian)

Zagorchev I (2007) Late Cenozoic development of the Strouma and Mesta fluviolacustrine systems, SW Bulgaria and northern Greece, Quaternary Science Reviews, 26 (22–24), 2783-2800, https://doi.org/10.1016/j.quascirev.2007.07.017.